



Plastic photodegradation under simulated marine conditions

Annalisa Delre^a, Maaike Goudriaan^a, Victor Hernando Morales^{a,b}, Annika Vaksmaa^a, Rachel Tintswalo Ndhlovu^a, Marianne Baas^a, Edwin Keijzer^a, Tim de Groot^a, Emna Zeghal^a, Matthias Egger^{c,d}, Thomas Röckmann^e, Helge Niemann^{a,f,g,*}

^a NIOZ Royal Netherlands Institute for Sea Research, Department of Marine Microbiology & Biogeochemistry, 't Horntje (Texel), the Netherlands

^b University of Vigo, Biological Oceanography Group, Vigo (Pontevedra), Spain

^c The Ocean Cleanup, Rotterdam, the Netherlands

^d Egger Research and Consulting, St. Gallen, Switzerland

^e Utrecht University, Faculty of Science, Institute for Marine and Atmospheric Research, Utrecht, the Netherlands

^f Utrecht University, Faculty of Geosciences, Department of Earth Sciences, Utrecht, the Netherlands

^g University of Tromsø, CAGE - Centre for Arctic Gas Hydrate, Environment and Climate, Tromsø, Norway

ARTICLE INFO

Keywords:

Microplastic
Photodegradation
Ocean plastic paradox

ABSTRACT

Ocean plastic pollution is a problem of increasing magnitude; yet, the amount of plastic at the sea surface is much lower than expected. Solar ultraviolet (UV) radiation can induce photodegradation, but its importance in determining the longevity of floating plastic remains unconstrained. Here, we measured photodegradation rates of different plastic types slightly larger than microplastics (virgin polymers and floating plastic debris) under simulated marine conditions. UV irradiation caused all plastic types to leach dissolved organic carbon, and to a lesser degree carbon dioxide, carbon monoxide, methane, and other hydrocarbon gases. The release of photodegradation products translates to degradation rates of 1.7–2.3 % yr⁻¹ of the tested plastic particles normalized to conditions as found in the subtropical surface ocean. Modelling the accumulation of floating plastic debris, our results show that solar UV radiation could already have degraded 7 to 22 % of all floating plastic that has ever been released to the sea.

1. Introduction

The amount of plastic entering the ocean is tightly coupled to the exponentially growing production of plastic (Jambeck et al., 2015; Wayman and Niemann, 2021) and corresponding indications for a growing ocean plastic budget were hence found (Lebreton et al., 2018; Ostle et al., 2019). However, the observed/inferred total amount of plastic marine debris (PMD) at the ocean surface is seemingly more than one order of magnitude lower compared to the expected mass of positively buoyant plastic released to the ocean since the 1950s, the onset of plastic mass production (Thompson et al., 2004; Wayman and Niemann, 2021). Several explanations were brought forward to explain the missing plastic paradox, which can be grouped in two categories: (i) Plastic transport from land to the sea is overestimated and (ii) processes removing plastic from the ocean surface are underestimated. (i) Rivers are considered as the main source of PMD, but riverine transport

(Lebreton et al., 2017; Meijer et al., 2021) might be overestimated (Weiss et al., 2021). Yet, atmospheric deposition of plastic is unaccounted for in current PMD budget estimates though this could be of a similar magnitude than all other land-sea plastic transport processes put together (Jambeck et al., 2015; Liss, 2020). (ii) Initially floating PMD can sink exporting plastic from the sea surface towards the ocean's interior (Woodall et al., 2014; Egger et al., 2020; Kane et al., 2020). Nevertheless, the composition of submerged and sedimented PMD is dominated by negatively buoyant plastic types, while PMD at the ocean surface is mostly comprised of polyethylene (PE) and polypropylene (PP) (Erni-Cassola et al., 2019; Egger et al., 2022). These plastic types are positively buoyant and thus more likely to remain at the ocean surface. PE and PP account for ≥50 % of the global plastic production (Geyer et al., 2017); selective removal of negatively buoyant plastic types alone can thus not explain the ocean plastic paradox. A more important factor in removing plastic from the ocean system appears to

* Corresponding author at: NIOZ Royal Netherlands Institute for Sea Research, Department of Marine Microbiology & Biogeochemistry, 't Horntje (Texel), the Netherlands.

E-mail address: helge.niemann@nioz.nl (H. Niemann).

<https://doi.org/10.1016/j.marpolbul.2022.114544>

Received 12 September 2022; Received in revised form 21 December 2022; Accepted 26 December 2022

Available online 12 January 2023

0025-326X/© 2023 The Authors. Published by Elsevier Ltd. This is an open access article under the CC BY license (<http://creativecommons.org/licenses/by/4.0/>).

be shore re-deposition (Lebreton et al., 2019; Onink et al., 2021). Models suggest that ~77 % of floating plastic remains in coastal areas and that a substantial fraction of this may beach within a few years after release (Onink et al., 2021). Floating PMD that has not beached is then transported offshore and accumulates in subtropical gyres and enclosed basins (Law et al., 2010; Cózar et al., 2014; van Sebille et al., 2015; Wayman and Niemann, 2021). There, additional degradation processes may further reduce the amount of floating PMD. This can be facilitated by microbes, heat and hydrolysis or photooxidation. The importance of microbial PMD degradation is discussed controversially (Vaksmas et al., 2021; Wayman and Niemann, 2021) and the rates of thermal degradation and hydrolyses are probably slow (Hakkarainen and Albertsson, 2004; Gardette et al., 2013; Gewert et al., 2015). In contrast, solar UV radiation is particularly strong in subtropical and tropical regions where floating PMD accumulates. The principals of photodegradation are reasonably well understood (Gewert et al., 2015; Andradý et al., 2022). UV radiation of plastics at the ocean surface initiates radical reactions that can lead to chain scission of the polymer and the release of organic and inorganic daughter products (Wayman and Niemann, 2021). This comprises compounds that remain as dissolved organic carbon (DOC) or dissolved inorganic carbon (DIC) in the aqueous phase as well as volatile molecules (e.g. short chain hydrocarbons) that typically escape to the gas phase. The velocity of photodegradation in the marine environment is not well constrained (Wayman and Niemann, 2021). Parametrisation of sinks for PMD is important to assess the fate and risks of plastic in the ocean, and to provide a baseline for well constrained policy strategies.

We investigated the release of photodegradation products of various plastic types during laboratory irradiation experiments simulating marine conditions. We quantified rates of photodegradation with the goal to estimate its importance for the longevity of floating PMD and the ocean plastic budget.

2. Materials and methods

2.1. Plastic types

Photodegradation experiments were conducted with the most important plastic types that are typically found at the ocean surface (Erni-Cassola et al., 2019): PE, PP, polystyrene (PS) and polyethylene-terephthalate (PET). We punched out discs of 6 mm diameter from 1 mm thick sheets of virgin polymers; low density PE, PP, PS, and PET (Goodfellow, UK: order Nrs. ET313010, PP303100, ST313120 and ES303010, respectively). Similarly, we also used 6 mm discs punched out of thinner (0.5 mm) sheets of PE (Goodfellow order Nr. ET311452) to compare photodegradation of standardized samples with different surface area to volume ratios. Finally, we also investigate photodegradation of PE and PP plastic marine debris (PMD) collected with a Manta trawl in the North Pacific subtropical gyre in November 2018 (Egger et al., 2020). The polymer identity was determined using Raman spectroscopy (Agiltron, INC.; PeakSeeker PEK-785). To ease comparability with the virgin plastics, we used polygon shaped, sheet-like pieces of ocean plastic that already featured similar surface area to volume ratios as the discs (Feret diameter: ~10 mm, thickness: 1 mm). Using pliers, we additionally broke down larger sheet-like 1 mm thick PMD fragments to pieces with a Feret diameter of ~10 mm. Particle geometries were determined through image analysis using the ImageJ software package. Prior to the experiment, all plastic pieces (virgin and PMD) were thoroughly rinsed with de-ionized water.

2.2. Irradiation experiments

To imitate solar radiation, we built a UV chamber comprising a housing made of stainless steel placed over a shaker table (Microplate Shaker TiMix control; Edmund Bühler, Germany; Goudriaan et al., 2023). Two fans facilitated constant convection to cool the system; the temperature inside the quartz bottles (see below) was maintained at

~45 °C throughout the duration of the irradiation experiment (the design of the UV chamber, i.e. power of light source and capacity of fans, did not allow to cool the system below this temperature). UV light was provided by a 460 W halogen metal-halide lamp (Supratec HTC 400241; Osram, Germany), that produces a UV spectrum similar to solar UV-A/B light with an intensity of 250 W m⁻² at the height of the plastic samples. Accounting for natural variations in solar radiation (day/night cycles, seasonal and meteorological variations), the average UV-A/B irradiance at the sea surface in temperate regions (~50°N/S), the subtropical (~30°N/S) and the tropical ocean (~equator) is ~10, ~25 and ~28 W m⁻², respectively (Li et al., 2015). 24 h exposure in the UV chamber was hence equivalent to ~25 average days of UV irradiance at the sea surface in temperate regions, ~10 days in subtropical regions, and ~9 days in the tropical ocean. We corrected photodegradation rates for temperature effects and production of degradation products in blank controls. We then normalized all photodegradation rates to subtropical ocean conditions.

For each type of virgin plastic, 47 discs with a total surface area of 35.4 cm² (6 mm diameter, 1 mm thickness) or 31 cm² (6 mm diameter, 0.5 mm thickness) were filled into 100 ml quartz bottles (Glasatelier Saillart; Belgium). Similarly, 1 g of polygon shaped PMD pieces (26 ± 5 ocean PE pieces, 33 ± 8 ocean PP pieces) with a total surface area of 30.8 ± 3.7 cm² (ocean PE) or 30.7 ± 1.4 cm² (ocean PP) were filled into the same type of bottle. To every bottle, 50 ml of filtered (0.2 µm) and sterilized seawater (autoclaved at 121 °C for 20 min) was added and the bottles were sealed with butyl rubber stoppers (RubberBv, The Netherlands). The bottles were irradiated upside down for the floating plastic types PE and PP, while bottles were kept in a tilted position for the non-buoyant plastic types PS and PET. All necks and bottle caps were wrapped with aluminium foil to prevent illumination of the butyl stoppers. To bottles/incubations with floating plastics, we additionally added 3 g of borosilicate glass beads (1 mm diameter; Glasgerätebau Ochs, Germany). These settled in the bottle neck and further shielded the butyl stoppers from UV light. We also incubated dark controls in the same way as light controls, but dark control bottles were fully wrapped in aluminium foil. Because the heat in the light controls was to a large degree the result of light absorbance by the sample water, we incubated dark controls in a heating cabinet at 45 °C. We also incubated blank controls only containing filtered sea water and glass beads in the same fashion as light controls.

Generally, each experiment lasted for a total of five days and was subsampled every ~24 h. Only the experiment with 0.5 mm thick PE discs was shorter (4 days) because of logistic reasons. At each time point, we removed 3 replicates of light and dark controls and one blank control from the UV chamber or heating cabinet, and measured headspace gases as well as DOC and DIC in the aqueous phase. Accumulation of carbon in the incubation vials of the light controls was corrected for blank and dark controls. Half-lives ($t_{1/2}$) were calculated for each plastic particle type assuming first order reaction kinetics (Ward et al., 2019; Zhu et al., 2020; Wayman and Niemann, 2021), i.e. plastic particle degradation follows exponential decay:

$$N_t = N_0 e^{-\lambda t} \quad (1)$$

and

$$N_t = N_0 - C_{ex} \quad (2)$$

where N_t is the amount of carbon remaining after time t , N_0 is the initial amount of carbon, λ is the degradation constant and C_{ex} is total carbon excess production, i.e., the sum of DOC, HC, CO, and DIC + CO₂ excess production. $t_{1/2}$ is then:

$$t_{1/2} = Ln(0.5)/\lambda \quad (3)$$

2.3. Analysis of head space gases and dissolved carbon

With an injection needle and gas-tight syringe, 1 ml of head space gases were sampled through the rubber stopper that seals the incubation bottles. The gases were then further analysed by gas chromatography (GC) with a methanizer and flame ionization detection (FID) and quadrupole mass spectrometry (MS). The GC unit consisted of an Agilent 7890B GC and gases were separated over an array of columns (HayeSep q 80/100 55 3 ft. 1/8 2 mm, Porapak q 6 ft. 1/8 2 mm, MolSieve 5A 60/88 55 8 ft. 2 mm). Concentrations of hydrocarbon gases, CO₂ and CO were determined by FID, which was calibrated with certified reference gases (Scott specialty gases, Air Liquide, Eindhoven, The Netherlands). The identity of gases was determined from their corresponding mass spectra (collected with an Agilent 5975C MS) and/or the retention times. The MS unit was also used to monitor O₂ to ensure that all photooxidation reactions proceeded at fully oxic conditions.

For dissolved phase analysis, the bottles were opened, and 5 ml of sample was taken immediately with a syringe for DIC analysis. This was filtered over GF/F inline filters (nominal mesh size = 0.7 μm; pre-combusted at 450 °C for 4 h) mounted in steel cartridges, and the effluent was collected headspace free in glass vials and analysed according to a method described previously (Stoll et al., 2001). For DOC analyses, an aliquot of 30 ml was filtered using pre-combusted (450 °C) GF/F inline filters and the effluent was collected in pre-combusted glass vials (EPA), acidified with concentrated HCl to pH <2 and stored at 4 °C until analysis. DOC was measured with a Shimadzu TOC-V VCSH with ASI-V auto sampler after removal of inorganic carbon by vigorous sparging with oxygen. The water was then injected onto a combustion column packed with platinum-coated alumina beads at 720 °C. Non-purgeable organic carbon compounds were combusted and converted to CO₂, which was then detected by a nondispersive infrared detector.

2.4. Accumulation of plastic in the ocean and importance of photodegradation

The amount of plastic entering the ocean is proportional to the global plastic production (Jambeck et al., 2015). For 2010, it has been estimated that 4.8 to 12.7 Mt of plastic waste entered the ocean (Jambeck et al., 2015), which is equivalent to 1.8–4.7 % of the annual plastic production of 2010 (PlasticsEurope, 2019). We modelled global plastic production for the years 1950 to 2018 by fitting market data (PlasticsEurope, 2019) polynomial (Fig. 2A). However, not all plastic types will remain afloat in the sea. PE and PP have densities lower than sea water and thus float at the ocean surface. PS, PET and most other plastic types have densities higher than sea water and thus only float if expanded or built to enclose larger volumes such as bottles. Consequently, floating PMD primarily comprises PE and PP, and only minor admixtures of PS, PET, and other plastic types (Erni-Cassola et al.,

2019). As a simplification of floating PMD, we thus only considered PE and PP, which account for 36 % (PE) and 21 % (PP) of the global plastic production (Geyer et al., 2017).

A likely important process removing plastic from the ocean is beaching, i.e. deposition of plastic at the shore line (Lebreton et al., 2019; Onink et al., 2021). Recent model estimations show that plastic input to the ocean mostly occurs in subtropical/tropical regions, that possibly ~77 % of floating plastic initially released to the sea remain in coastal zones and that >30 % probably beaches within a time span of ~5 years after release (Onink et al., 2021). As a simplification for beaching, we calculated that (a) 30 % of the initially released floating PMD is immediately redeposited at the shore and thus removed from the ocean. In a second scenario, (b) we considered that all floating plastic remaining in coastal zones (77 % of the initially released floating plastic) beaches instantaneously.

We calculated photodegradation of the remaining floating PMD for UV conditions as are found in the subtropical ocean (Li et al., 2015), because floating PMD seemingly accumulates in the subtropical ocean gyres or remains in the subtropical/tropical coastal seas (van Sebille et al., 2015; Onink et al., 2021). For this, we considered an average degradation rate for PE (1.8 % yr⁻¹; t_{1/2} = 38.4 yrs) in accordance with our measurements for virgin (1.81 ± 0.14 % yr⁻¹; t_{1/2} = 37.95 yrs) and PMD particles (1.78 ± 0.56 % yr⁻¹; t_{1/2} = 38.6 yrs) and a degradation rate for PP based on our measurements for virgin PP (4.18 % yr⁻¹; t_{1/2} = 16.2 yrs). We did not consider ocean PP because of the non-linear degradation of PP PMD in our experiments. The total amount of either PE or PP after a given year (PE_t, PP_t) can then be calculated as:

$$(PE_t, PP_t) = (PE_{t-1}, PP_{t-1}) e^{-\lambda t} + (PE_{in}, PP_{in}) \quad (4)$$

where λ is the degradation constant (see Eq. (1)), (PE_{t-1}, PP_{t-1}) is the residual amount of PE or PP (i.e. the accumulated mass of PMD that has remained after beaching and photodegradation in the previous year) and (PE_{in}, PP_{in}) is the input of new PE or PP (i.e. PE and PP transported from land to the sea, and remaining in the ocean after beaching during a given year). Because the time interval for each model step was one year, t was set to 1. (PE_{in}, PP_{in}) was determined as:

$$(PE_{in}, PP_{in}) = GPP_t \times (PE_{MS}, PP_{MS}) \times f_R \times (1 - f_B) \quad (5)$$

where GPP_t is the global plastic production during a given year (determined from our model fit for global production figures), (PE_{MS}, PP_{MS}) is the market share of PE or PP (0.36 and 0.21 respectively), f_R is the fraction of the global plastic production that is released to the ocean (0.018 and 0.047) and f_B is the fraction of PMD that beaches (0.3 and 0.77). For the first time interval, 1950–1951, (PE_t, PP_t) was (PE_{in}, PP_{in}) for the year 1950.

Table 1

Tested plastic types and photodegradation rates under simulated marine conditions. Photodegradation rates (for virgin polymers and plastics collected from the North Pacific subtropical gyre - NPSG) are normalized to subtropical marine conditions. Values are presented per plastic piece (circular disc of virgin plastic, polygon flake of plastic marine debris - PMD). Standard errors are indicated for average values of mass and degradation rates (mg-C cm⁻² yr⁻¹, % yr⁻¹). Degradation metrics are normalized to subtropical ocean surface conditions. Degradation rates of ocean PP could not be determined from linear regression analysis. Abbreviations: SA = surface area, Z = thickness, nd = not determined.

polymer	origin	shape	SA(cm ²)	Z (mm)	Mass (mg)	Degradation		
						mg-C cm ⁻² yr ⁻¹	% yr ⁻¹	t _{1/2} (yr)
PE	virgin	disc	0.75	1.0	27.41 ± 0.0	0.66 ± 0.05	1.81 ± 0.14	37.9 (35.2–41.2)
	virgin	disc	0.66	0.5	14.21 ± 0.1	0.50 ± 0.03	2.31 ± 0.16	29.7 (27.7–31.9)
	NPSG	polygon	1.22 ± 0.12	~1	38.46 ± 7.5	0.63 ± 0.13	1.78 ± 0.56	38.6 (29.3–56.5)
PP	virgin	disc	0.75	1.0	25.41 ± 0.0	1.41 ± 0.16	4.18 ± 0.47	16.2 (14.6–18.3)
	NPSG	polygon	0.97 ± 0.23	~1	30.06 ± 7.2	nd	nd	nd
PS	virgin	disc	0.75	1.0	38.33 ± 0.0	0.97 ± 0.10	1.99 ± 0.20	34.5 (31.3–38.4)
PET	virgin	disc	0.75	1.0	38.55 ± 0.0	0.85 ± 0.11	1.65 ± 0.21	44.4 (36.9–47.8)

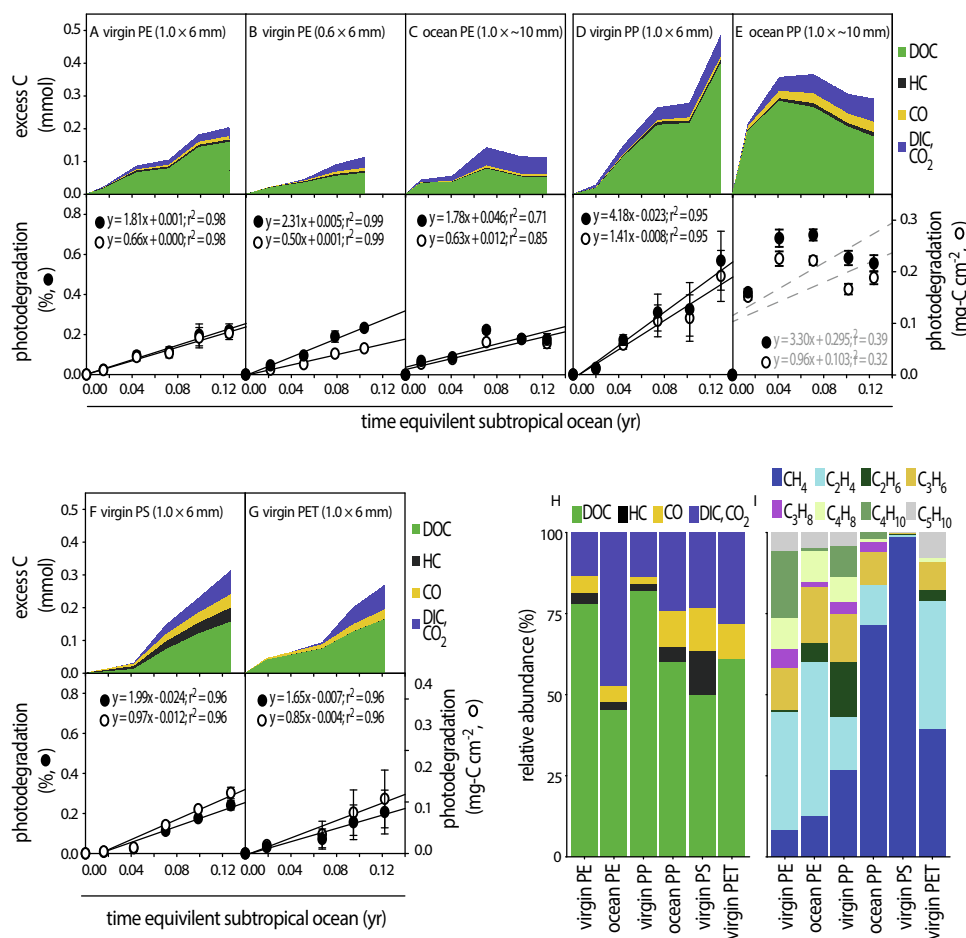


Fig. 1. Release of photodegradation products from PE (A, B, C), PP (D, E), PS (F) and PET (G) upon irradiation with UV light. The accumulation of gaseous and dissolved photodegradation products (upper panels) translates to linear degradation rates of the standardized discs of virgin plastics (lower panels; normalized to mass (%-degradation) or surface area). In accordance with a higher surface area to volume ratio, %-degradation of thinner PE discs (B), was much higher than that of the thicker PE discs, while degradation per surface area was similar. Degradation of PMD was more variable; in particular ocean PP degradation did not follow linear trends within the duration of our experiments (indicated by grey font type and lines, cf. supplementary Fig. 1). Degradation time is normalized to UV irradiation intensity as found in the subtropical ocean surface. Relative composition of all degradation products (H) and hydrocarbon gases, only (I).

3. Results and discussion

3.1. Release of photodegradation products under simulated marine conditions

In this work, different types of plastic were irradiated with UV light under simulated marine conditions. The plastic types were commercially available virgin PE and PP as representatives for floating plastics, PS and PET as non-floating plastics, as well as PE and PP fragments recovered as floating PMD from the North Pacific subtropical gyre (Table 1). In the ocean, floating PMD is predominantly composed of PE (>50 %) and PP (>30 %) (Erni-Cassola et al., 2019). All plastic types tested here released a variety of degradation products upon exposure to UV radiation (Fig. 1). Organic carbon compounds accounted for the majority, i.e. 47–84 % of all carbon in the pool of photodegradation products. These comprised small molecules and fragments (<0.7 μm) that we measured collectively as DOC in the water, and hydrocarbon gases such as methane, which accumulated in the head space air of the quartz vials in which the plastic fragments were irradiated (Fig. 1). Other degradation products were CO, accounting for <13 %, and the terminal oxidation products CO_2 and DIC accounting for 13–47 % of all carbon compounds.

We found that thermal degradation alone (45 °C dark incubations) caused high rates of DOC release from PMD (collected from the marine environment) accounting for 35 (ocean PE) to 66 % (ocean PP) of total DOC production, while this was <8 % for all virgin polymers (supplementary Fig. 1, supplementary table 1). We attribute the higher DOC release from PMD to the advanced state of (photo)degradation of the PMD polymer matrix, probably comprising already fragmented carbon chains, which are more likely to release degradation products (Gewert et al., 2018; Romera-Castillo et al., 2022a). Also, potential additives in

the PMD might have caused the higher release rates of DOC (Walsh et al., 2021). For quantification of photodegradation, we corrected degradation rates for the temperature effect. For the ocean PP particles, this was higher than the UV effect, leading to a seemingly decreasing accumulation of photodegradation products (Fig. 1E, supplementary fig. 1). We did thus not consider results from our experiments with ocean PP for the further evaluation of the quantitative importance of photodegradation in removing floating PMD from the ocean surface. Nevertheless, our results indicate that thermal degradation of weathered and partially degraded floating PMD might be important in the subtropical/tropical ocean where sea surface temperatures can be high (>30 °C; Good et al., 2020).

3.2. Photodegradation rates

Accumulation of photodegradation products from polymer types tested here (not considering ocean PP) followed linear trends and amounted to ≥ 0.2 % of the initial polymer-bound carbon within the time of the experiment (Fig. 1). Previous studies measuring single types of photodegradation products, DOC from PE (Zhu et al., 2020), PS (Ward et al., 2019) and mixed PMD (Zhu et al., 2020), and hydrocarbon gases released from PE (Royer et al., 2018), found linear release rates, too. Exceptionally, increasing rates of DOC release from PE, PP and PS were also reported (Zhu et al., 2020). Normalized to environmental conditions as encountered at the subtropical ocean surface, accumulation of photodegradation products in our experiments translates to photodegradation rates of the tested plastic pieces of ≥ 1.65 % yr^{-1} (Fig. 1). This is equivalent to half-lives of ≤ 41.7 yrs (Table 1). Photodegradation-induced DOC release from different plastic types normalized to subtropical UV levels in other studies (Ward et al., 2019; Zhu et al., 2020;

Wayman and Niemann, 2021; Romera-Castillo et al., 2022a) were similar to our results. Romera-Castillo et al. (2022a) found, however, an even higher offset in DOC release when comparing virgin plastic and PMD.

We found that the percent-degradation of the smaller PE disks was higher when compared to the larger counterparts, while rates of photodegradation normalized to surface area was similar (Table 1, Fig. 1A, B). Photodegradation is mostly confined to the particle surface where UV photons are absorbed (Gewert et al., 2015; ter Halle et al., 2016; Andradý et al., 2022). Consequently, small particles with a high surface area to volume ratio degrade faster than larger particles with a lower surface area to volume ratio. The commercial plastic types used here were circular discs (6 mm diameter) and the PMD fragments were polygon shaped (~10 mm Feret diameter); both fragment shapes are thus slightly larger than microplastic (≤ 5 mm). The majority of floating PMD particles in the ocean is $\ll 5$ mm (Poulain et al., 2019; Lindeque et al., 2020), thus smaller and characterised by a higher surface area to volume ratio than the particles investigated here. This suggests that the photodegradation rates presented in this study are a conservative estimate for photodegradation of PMD microplastic pieces floating in the subtropical/tropical ocean.

To assess the possible contribution of photodegradation to the marine missing plastics paradox, we constructed a discrete-time model of floating PMD accumulation at the ocean surface. The model incorporates rates of plastic input to the ocean (Jambeck et al., 2015) (Fig. 2A) - and as processes removing PMD from the ocean surface, beaching (Onink et al., 2021) and photodegradation (Table 1, Fig. 1). Note that this model is simplified in considering that beaching occurs immediately after plastic release and permanently removes plastic from the ocean system. The model does also not account for sinking and microbial degradation, which also remove at least some PMD from the ocean surface (Wayman and Niemann, 2021). We also simplified floating PMD to PE and PP as these constitute the most important fractions of floating PMD (Erni-Cassola et al., 2019). The model shows that plastic accumulates exponentially in the ocean though at differential rates depending on the strength of the removal processes (Fig. 2B, C). It also shows that ongoing photodegradation of the residual floating PMD in the range of a few yr^{-1} (in accordance with our measurement

results; Table 1) can substantially reduce accumulation of floating PMD. Depending on the initial removal rate due to beaching (77 and 30 %, respectively), photodegradation in our model runs accounted for ~7 % to up to 22 % removal of all floating plastic that has been released to the ocean since the 1950s when plastic mass production started.

3.3. Potential impact and fate of photodegradation products in the ocean

Photodegradation induced by solar UV light can apparently remove a substantial fraction of floating PMD, converting it to DOC (typically >50 %), DIC (typically <50 %) as well as hydrocarbon gases and CO (typically <10 %) (see above). This begs the question: what are the potential impacts of daughter products from PMD photodegradation on the marine environment?

For the year 2018 alone, our model predicts that solar UV light degraded 0.54 to 1.64 Mt PMD (when considering a beaching rate of 77 and 30 %, respectively). The release of hydrocarbon gases and CO would hence amount to ≤ 0.1 Mt yr^{-1} , mostly being liberated to the atmosphere. There, hydrocarbon gases and CO contribute to the greenhouse effect (IPCC, 2021). Nevertheless, the additional input of these gases from photodegradation of floating PMD seems small when considering the global inputs methane (one of the most important greenhouse gases, 576–737 Mt yr^{-1} ; Saunio et al., 2019) and CO to the atmosphere (~2600 Mt yr^{-1} ; Zheng et al., 2019). The mass of DOC and DIC released from PMD would amount to ≤ 1 Mt yr^{-1} , but just as for hydrocarbon gases and CO, this seems small when compared to the total DOC and DIC budgets of the surface ocean (25,000 Mt and 700,000 Mt, respectively; Houghton, 2014). Nevertheless, locally, PMD photodegradation might lead to transiently elevated DOC and DIC levels in waters directly adjacent to the PMD fragments. DIC and some DOC compounds (e.g. carboxylic acids) can increase the acidity of ocean water (Romera-Castillo et al., 2022b), which has potentially negative consequences for marine life in habitats adjacent to floating PMD fragments. Plastic-derived DOC will, at least in parts, be utilized by marine microorganisms (Romera-Castillo et al., 2018, 2022a, 2022c; Zhu et al., 2020; Vaksmaa et al., 2021). Nevertheless, DOC released upon photodegradation and fragmentation of PMD comprises a broad variety of compounds ranging from more bioavailable smaller organic molecules to complex and potentially more recalcitrant fragments including nanoplastics (Gewert et al., 2015, 2018; Lambert and Wagner, 2016; Ward et al., 2019; Enfrin et al., 2020; Menzel et al., 2022). Nanoplastics were found in the coastal and the open ocean (ter Halle et al., 2017; Materić et al., 2022). They likely have adverse effects on aquatic organisms (Mattsson et al., 2017; Jeong et al., 2018; Baudrimont et al., 2020; Wayman and Niemann, 2021) and it is unclear if nanoplastics can be degraded by microorganism (Sharma et al., 2022).

4. Summary and conclusions

This study investigated kinetics of photodegradation of common plastic types found afloat at the ocean surface. Normalized to conditions as encountered at the sea surface in subtropical latitudes, our results show that UV light degrades larger microplastic particles by >1.7 % yr^{-1} (equivalent to half lives <44.4 yrs). In a simplified model, this suggest that up to 22 % of all floating plastic ever released to the ocean could have been degraded by solar UV radiation. Photodegradation is thus an apparent key sink mechanism for floating PMD and could explain a substantial part of the missing plastic paradox. Nevertheless, our study also shows that photodegradation mostly transforms plastic polymers to smaller organic carbon compounds (DOC and hydrocarbons) rather than fully mineralizing plastic to DIC and CO_2 . The impacts of photodegradation-induced release of DOC and DIC from PMD to the marine environment are not well constrained. Photodegradation-derived DOC comprises a broad range of compounds including nanoplastics. Photodegradation could thus lead to elevated concentrations of nanoplastics in the subtropical and tropical ocean where plastics

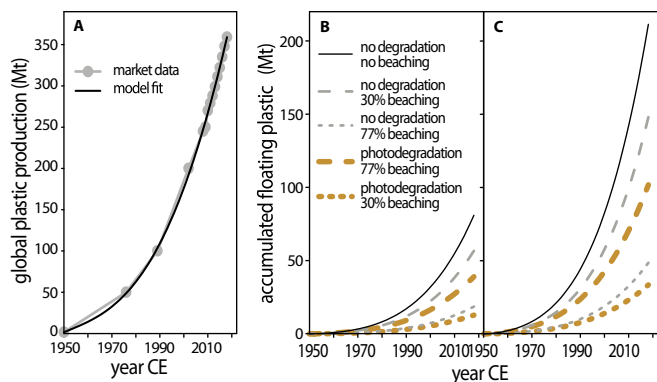


Fig. 2. (A) Market data of global plastic production and polynomial fit ($y = -0.000003 \times x^4 + 0.001161 \times x^3 - 0.003380 \times x^2 + 1.182973 \times x + 1.562761$, $r^2 = 0.99$). Modelled accumulation of floating PMD (simplified to PE and PP) considering that 1.8 % (B) to 4.7 % (C) of the global plastic production is released to the ocean. Different accumulation scenarios, without and with sink mechanisms (beaching, beaching and photodegradation), are highlighted. Without any sink mechanism, floating PMD amounts to 81–211 Mt in 2018 (solid black line). Subsequently to the release of plastic to the ocean, beaching reduces the mass of floating PMD by 30–77 % (dashed and dotted grey lines). Ongoing photodegradation further reduces the mass of floating PMD remaining after beaching by 31 % (dashed and dotted orange lines). Depending on the initial beaching rate, this is equivalent to 7–22 % of the mass of floating plastic that has ever been released to the sea.

accumulate, which has unforeseeable consequences for marine life in these ecosystems.

CRedit authorship contribution statement

Annalisa Delre: Conceptualization, Investigation, Visualization, Writing – original draft, Writing – review & editing. **Maaike Goudriaan:** Conceptualization, Writing – review & editing. **Victor Hernandez Morales:** Conceptualization, Methodology, Writing – review & editing. **Annika Vaksmaa:** Conceptualization, Methodology, Writing – review & editing. **Rachel Tintswalo Ndhlovu:** Methodology, Investigation, Writing – review & editing. **Marianne Baas:** Methodology, Writing – review & editing. **Edwin Keijzer:** Methodology, Writing – review & editing. **Tim de Groot:** Methodology, Writing – review & editing. **Emma Zeghal:** Methodology, Writing – review & editing. **Matthias Egger:** Methodology, Writing – review & editing. **Thomas Röckmann:** Writing – review & editing. **Helge Niemann:** Conceptualization, Visualization, Funding acquisition, Project administration, Supervision, Writing – original draft, Writing – review & editing.

Declaration of Competing Interest

The authors declare that they have no known competing financial interests or personal relationships that could have appeared to influence the work reported in this paper.

Data availability

All data will be archived and made publicly available in the data base DAS (Data Archive System, www.nioz.nl/en/research/dataportal/das).

Acknowledgments

We thank captain and crew, and shipboard scientific party of the Maersk Transporter. We are grateful to Marcel van der Meer, Sharyn and Jort Ossebaar, Ronald van Bommel and Karel Bakker for technical assistance. This work has been supported by the European Research Council (ERC-CoG grant no. 772923, project VORTEX) and the Dutch Research Council (grant no. OCENW.XS2.018).

Appendix A. Supplementary data

Supplementary data to this article can be found online at <https://doi.org/10.1016/j.marpolbul.2022.114544>.

References

- Andrady, A.L., Law, K.L., Donohue, J., Koongolla, B., 2022. Accelerated degradation of low-density polyethylene in air and in sea water. *Sci. Total Environ.* 811, 151368 <https://doi.org/10.1016/j.scitotenv.2021.151368>.
- Baudrimont, M., Arini, A., Guégan, C., Venel, Z., Gigault, J., Pedrono, B., Prunier, J., Maurice, L., ter Halle, A., Feurtet-Mazel, A., 2020. Ecotoxicity of polyethylene nanoplastics from the North Atlantic oceanic gyre on freshwater and marine organisms (microalgae and filter-feeding bivalves). *Environ. Sci. Pollut. Res.* 27, 3746–3755. <https://doi.org/10.1007/s11356-019-04668-3>.
- Cózar, A., Echevarría, F., González-Gordillo, J.L., Irigoien, X., Ubeda, B., Hernández-León, S., Palma, A.T., Navarro, S., García-de-Lomas, J., Ruiz, A., Fernández-de-Puelles, M.L., Duarte, C.M., 2014. Plastic debris in the open ocean. *Proc. Natl. Acad. Sci.* 111, 10239–10244. <https://doi.org/10.1073/pnas.1314705111>.
- Egger, M., Sulu-Gambari, F., Lebreton, L., 2020. First evidence of plastic fallout from the North Pacific garbage patch. *Sci. Rep. UK* 10, 7495. <https://doi.org/10.1038/s41598-020-64465-8>.
- Egger, M., Schilt, B., Wolter, H., Mani, T., de Vries, R., Zettler, E., Niemann, H., 2022. Pelagic distribution of plastic debris (> 500 µm) and marine organisms in the upper layer of the North Atlantic Ocean. *Sci Rep-uk* 12, 13465. <https://doi.org/10.1038/s41598-022-17742-7>.
- Enfrin, M., Lee, J., Gibert, Y., Basheer, F., Kong, L., Dumée, L.F., 2020. Release of hazardous nanoplastic contaminants due to microplastics fragmentation under shear stress forces. *J. Hazard. Mater.* 384 <https://doi.org/10.1016/j.jhazmat.2019.121393>.

- Erni-Cassola, G., Zadjelovic, V., Gibson, M.I., Christie-Oleza, J.A., 2019. Distribution of plastic polymer types in the marine environment; a meta-analysis. *J. Hazard. Mater.* 369, 691–698. <https://doi.org/10.1016/j.jhazmat.2019.02.067>.
- Gardette, M., Perthue, A., Gardette, J.-L., Janecska, T., Földes, E., Pukánszky, B., Therias, S., 2013. Photo- and thermal-oxidation of polyethylene: comparison of mechanisms and influence of unsaturation content. *Polym. Degrad. Stabil.* 98, 2383–2390. <https://doi.org/10.1016/j.polydegradstab.2013.07.017>.
- Gewert, B., Plassmann, M.M., MacLeod, M., 2015. Pathways for degradation of plastic polymers floating in the marine environment. *Environ. Sci. Process. Impacts* 17, 1513–1521. <https://doi.org/10.1039/c5em00207a>.
- Gewert, B., Plassmann, M., Sandblom, O., MacLeod, M., 2018. Identification of chain scission products released to water by plastic exposed to ultraviolet light. *Environ. Sci. Technol. Lett.* 5, 272–276. <https://doi.org/10.1021/acs.estlett.8b00119>.
- Geyer, R., Jambeck, J.R., Law, K.L., 2017. Production, use, and fate of all plastics ever made. *Sci. Adv.* 3, e1700782 <https://doi.org/10.1126/sciadv.1700782>.
- Good, S., Fiedler, E., Mao, C., Martin, M.J., Maycock, A., Reid, R., Roberts-Jones, J., Searle, T., Waters, J., While, J., Worsfold, M., 2020. The current configuration of the OSTIA system for operational production of Foundation Sea surface temperature and ice concentration analyses. *Remote Sens. (Basel)* 12, 720. <https://doi.org/10.3390/rs12040720>.
- Goudriaan, M., Morales, V.H., van der Meer, M.T.J., Mets, A., Ndhlovu, R.T., van Heerwaarden, J., Simon, S., Heuer, V.B., Hinrichs, K.-U., Niemann, H., 2023. A stable isotope assay with ¹³C-labeled polyethylene to investigate plastic mineralization mediated by rhodococcus ruber. *Mar. Pollut. Bull.* 186, 114369. <https://doi.org/10.1016/j.marpolbul.2022.114369>.
- Hakkarainen, M., Albertsson, A.-C., 2004. Environmental degradation of polyethylene. In: Albertsson, A.-C. (Ed.), *Long Term Properties of Polyolefins*. Springer, Berlin Heidelberg, Berlin, Heidelberg, pp. 177–200. <https://doi.org/10.1007/b13523>.
- Houghton, R.A., 2014. The contemporary carbon cycle. In: Holland, H.D., Turekian, K.K. (Eds.), *Treatise on Geochemistry*. Elsevier, pp. 399–435. <https://doi.org/10.1016/b978-0-08-095975-7.00810-x>.
- IPCC, 2021. *Climate Change 2021: The Physical Science Basis. Contribution of Working Group I to the Sixth Assessment Report of the Intergovernmental Panel on Climate Change*. Chemistry International. Cambridge University Press, Cambridge, United Kingdom and New York, NY, USA. <https://doi.org/10.1515/ci-2021-0407>.
- Jambeck, J.R., Geyer, R., Wilcox, C., Siegler, T.R., Perryman, M., Andrady, A., Narayan, R., Law, K.L., 2015. Marine pollution. Plastic waste inputs from land into the ocean. *Science* 347, 768–771. <https://doi.org/10.1126/science.1260352>.
- Jeong, C.-B., Kang, H.-M., Lee, Y.H., Kim, M.-S., Lee, Jin-Sol, Seo, J.S., Wang, M., Lee, Jae-Seong, 2018. Nanoplastic ingestion enhances toxicity of persistent organic pollutants (POPs) in the monogonot rotifer *Brachionus koreanus* via multixenobiotic resistance (MXR) disruption. *Environ Sci Technol* 52, 11411–11418. <https://doi.org/10.1021/acs.est.8b03211>.
- Kane, I.A., Clare, M.A., Miramontes, E., Wogelius, R., Rothwell, J.J., Garreau, P., Pohl, F., 2020. Seafloor microplastic hotspots controlled by deep-sea circulation. *Science* 368, 1140–1145. <https://doi.org/10.1126/science.aba5899>.
- Lambert, S., Wagner, M., 2016. Characterisation of nanoplastics during the degradation of polystyrene. *Chemosphere* 145, 265–268. <https://doi.org/10.1016/j.chemosphere.2015.11.078>.
- Law, K.L., Moré-Ferguson, S., Maximenko, N.A., Proskurowski, G., Peacock, E.E., Hafner, J., Reddy, C.M., 2010. Plastic accumulation in the North Atlantic subtropical gyre. *Science* 329, 1185–1188. <https://doi.org/10.1126/science.1192321>.
- Lebreton, L.C.M., van der Zwet, J., Damsteeg, J.-W., Slat, B., Andrady, A., Reisser, J., 2017. River plastic emissions to the world's oceans. *Nat. Commun.* 8, 1–10. <https://doi.org/10.1038/ncomms15611>.
- Lebreton, L., Slat, B., Ferrari, F., Sainte-Rose, B., Aitken, J., Marthouse, R., Hajbane, S., Cunsolo, S., Schwarz, A., Levivier, A., Noble, K., Debeljak, P., Maral, H., Schoeneich-Argent, R., Brambini, R., Reisser, J., 2018. Evidence that the great Pacific garbage patch is rapidly accumulating plastic. *Sci. Rep. UK* 8, 4666. <https://doi.org/10.1038/s41598-018-22939-w>.
- Lebreton, L., Egger, M., Slat, B., 2019. A global mass budget for positively buoyant macroplastic debris in the ocean. *Sci. Rep. UK* 9, 12922. <https://doi.org/10.1038/s41598-019-49413-5>.
- Li, T., Pan, D., Bai, Y., Li, G., He, X., Chen, C.-T.A., Gao, K., Liu, D., Lei, H., 2015. Satellite remote sensing of ultraviolet irradiance on the ocean surface. *Acta Oceanol. Sin.* 34, 101–112. <https://doi.org/10.1007/s13131-015-0690-z>.
- Lindeque, P.K., Cole, M., Coppock, R.L., Lewis, C.N., Miller, R.Z., Watts, A.J.R., Wilson-McNeal, A., Wright, S.L., Galloway, T.S., 2020. Are we underestimating microplastic abundance in the marine environment? A comparison of microplastic capture with nets of different mesh-size. *Environ. Pollut.* 265, 114721. <https://doi.org/10.1016/j.envpol.2020.114721>.
- Liss, P.S., 2020. Microplastics: all up in the air? *Mar. Pollut. Bull.* 153, 110952. <https://doi.org/10.1016/j.marpolbul.2020.110952>.
- Materić, D., Holzinger, R., Niemann, H., 2022. Nanoplastics and ultrafine microplastic in the dutch Wadden Sea - the hidden plastics debris? *Sci. Total Environ.* 846, 157371. <https://doi.org/10.1016/j.scitotenv.2022.157371>.
- Mattsson, K., Johnson, E.V., Malmendal, A., Linse, S., Hansson, L.-A., Cedervall, T., 2017. Brain damage and behavioural disorders in fish induced by plastic nanoparticles delivered through the food chain. *Sci. Rep.-UK* 7. <https://doi.org/10.1038/s41598-017-10813-0>.
- Meijer, L.J.J., van Emmerik, T., van der Ent, R., Schmidt, C., Lebreton, L., 2021. More than 1000 rivers account for 80% of global riverine plastic emissions into the ocean. *Sci. Adv.* 7, eaaz5803. <https://doi.org/10.1126/sciadv.aaz5803>.
- Menzel, T., Meides, N., Mauel, A., Mansfeld, U., Kretschmer, W., Kuhn, M., Herzig, E.M., Altstädt, V., Strohriegel, P., Senker, J., Ruckdäschel, H., 2022. Degradation of low-

- density polyethylene to nanoplastic particles by accelerated weathering. *Sci. Total Environ.* 826, 154035 <https://doi.org/10.1016/j.scitotenv.2022.154035>.
- Onink, V., Jongedijk, C.E., Hoffman, M.J., van Seville, E., Laufkötter, C., 2021. Global simulations of marine plastic transport show plastic trapping in coastal zones. *Environ. Res. Lett.* 16, 064053 <https://doi.org/10.1088/1748-9326/abcabd>.
- Ostle, C., Thompson, R.C., Broughton, D., Gregory, L., Wootton, M., Johns, D.G., 2019. The rise in ocean plastics evidenced from a 60-year time series. *Nat. Commun.* 10, 1622. <https://doi.org/10.1038/s41467-019-09506-1>.
- PlasticsEurope, 2019. *Plastics—The Facts 2019: An Analysis of European Plastics Production, Demand and Waste Data*. PlasticsEurope.
- Poulain, M., Mercier, M.J., Brach, L., Martignac, M., Routaboul, C., Perez, E., Desjean, M. C., ter Halle, A., 2019. Small microplastics as a main contributor to plastic mass balance in the North Atlantic subtropical gyre. *Environ. Sci. Technol.* 53, 1157–1164. <https://doi.org/10.1021/acs.est.8b05458>.
- Romera-Castillo, C., Pinto, M., Langer, T.M., Álvarez-Salgado, X.A., Herndl, G.J., 2018. Dissolved organic carbon leaching from plastics stimulates microbial activity in the ocean. *Nat. Commun.* 9, 1–7. <https://doi.org/10.1038/s41467-018-03798-5>.
- Romera-Castillo, C., Birnstiel, S., Álvarez-Salgado, X.A., Sebastián, M., 2022a. Aged plastic leaching of dissolved organic matter is two orders of magnitude higher than virgin plastic leading to a strong uplift in marine microbial activity. *Frontiers Mar Sci* 9, 861557. <https://doi.org/10.3389/fmars.2022.861557>.
- Romera-Castillo, C., Lucas, A., Mallenco-Fornies, R., Briones-Rizo, M., Calvo, E., Pelejero, C., 2022b. Abiotic plastic leaching contributes to ocean acidification. *Sci. Total Environ.* 854, 158683 <https://doi.org/10.1016/j.scitotenv.2022.158683>.
- Romera-Castillo, C., Mallenco-Fornies, R., Saá-Yáñez, M., Xosé, A.Á.-S., 2022c. Leaching and bioavailability of dissolved organic matter from petrol-based and biodegradable plastics. *Mar. Environ. Res.* 176, 105607 <https://doi.org/10.1016/j.marenvres.2022.105607>.
- Royer, S.-J., Ferrón, S., Wilson, S.T., Karl, D.M., Pardha-Saradhi, P., 2018. Production of methane and ethylene from plastic in the environment. *Plos One* 13, e0200574. <https://doi.org/10.1371/journal.pone.0200574>.
- Saunois, M., Staver, A.R., Poulter, B., Bousquet, P., Canadell, J.G., Jackson, R.B., Raymond, P.A., Dlugokencky, E.J., Houweling, S., Patra, P.K., Ciais, P., Arora, V.K., Bastviken, D., Bergamaschi, P., Blake, D.R., Brailsford, G., Bruhwiler, L., Carlson, K. M., Carrol, M., Castaldi, S., Chandra, N., Crevoisier, C., Crill, P.M., Covey, K., Curry, C.L., Etiope, G., Frankenberg, C., Gedney, N., Hegglin, M.I., Höglund-Isaksson, L., Hugelius, G., Ishizawa, M., Ito, A., Janssens-Maenhout, G., Jensen, K.M., Joos, F., Kleinen, T., Krummel, P.B., Langenfelds, R.L., Laruelle, G.G., Liu, L., Machida, T., Maksyutov, S., McDonald, K.C., McNorton, J., Miller, P.A., Melton, J.R., Morino, I., Müller, J., Murgia-Flores, F., Naik, V., Niwa, Y., Noce, S., O'Doherty, S., Parker, R.J., Peng, C., Peng, S., Peters, G.P., Prigent, C., Prinn, R., Ramonet, M., Regnier, P., Riley, W.J., Rosentretter, J.A., Segers, A., Simpson, I.J., Shi, H., Smith, S. J., Steele, L.P., Thornton, B.F., Tian, H., Tohjima, Y., Tubiello, F.N., Tsuruta, A., Viovy, N., Voulgarakis, A., Weber, T.S., van Weele, M., van der Werf, G.R., Weiss, R. F., Worthy, D., Wunch, D., Yin, Y., Yoshida, Y., Zhang, W., Zhang, Z., Zhao, Y., Zheng, B., Zhu, Qing, Zhu, Qiu, Q., 2019. The global methane budget 2000–2017. *Earth Syst. Sci. Data Discuss.* 1–138 <https://doi.org/10.5194/essd-2019-128>.
- Sharma, V.K., Ma, X., Lichtfouse, E., Robert, D., 2022. Nanoplastics are potentially more dangerous than microplastics. *Environ. Chem. Lett.* 1–4 <https://doi.org/10.1007/s10311-022-01539-1>.
- Stoll, M.H.C., Bakker, K., Nobbe, G.H., Haese, R.R., 2001. Continuous-flow analysis of dissolved inorganic carbon content in seawater. *Anal. Chem.* 73, 4111–4116. <https://doi.org/10.1021/ac010303r>.
- ter Halle, A., Ladirat, L., Gendre, X., Goudouneche, D., Pusineri, C., Routaboul, C., Tenailleu, C., Duployer, B., Perez, E., 2016. Understanding the fragmentation pattern of marine plastic debris. *Environ. Sci. Technol.* 50, 5668–5675. <https://doi.org/10.1021/acs.est.6b00594>.
- ter Halle, A., Jeanneau, L., Martignac, M., Jardé, E., Pedrono, B., Brach, L., Gigault, J., 2017. Nanoplastic in the North Atlantic subtropical gyre. *Environ. Sci. Technol.* 51, 13689–13697. <https://doi.org/10.1021/acs.est.7b03667>.
- Thompson, R.C., Olsen, Y., Mitchell, R.P., Davis, A., Rowland, S.J., John, A.W.G., McGonigle, D., Russell, A.E., 2004. Lost at sea: where is all the plastic? *Science* 304, 838. <https://doi.org/10.1126/science.1094559>.
- Vaksmas, A., Hernando-Morales, V., Zeghal, E., Niemann, H., 2021. Microbial degradation of marine plastics: current state and future prospects. In: Joshi, S.J., Deshmukh, A., Sarma, H. (Eds.), *Biotechnology for Sustainable Environment*. Springer, Singapore, pp. 111–154. https://doi.org/10.1007/978-981-16-1955-7_5.
- van Seville, E., Wilcox, C., Lebreton, L., Maximenko, N., Hardesty, B.D., van Franeker, J. A., Eriksen, M., Siegel, D., Galgani, F., Law, K.L., 2015. A global inventory of small floating plastic debris. *Environ. Res. Lett.* 10, 124006 <https://doi.org/10.1088/1748-9326/10/12/124006>.
- Walsh, A.N., Reddy, C.M., Niles, S.F., McKenna, A.M., Hansel, C.M., Ward, C.P., 2021. Plastic formulation is an emerging control of its photochemical fate in the ocean. *Environ. Sci. Technol.* <https://doi.org/10.1021/acs.est.1c02272>.
- Ward, C.P., Armstrong, C.J., Walsh, A.N., Jackson, J.H., Reddy, C.M., 2019. Sunlight converts polystyrene to carbon dioxide and dissolved organic carbon. *Environ. Sci. Technol. Lett.* 6, 669–674. <https://doi.org/10.1021/acs.estlett.9b00532>.
- Wayman, C., Niemann, H., 2021. The fate of plastic in the ocean environment – a minireview. *Environmental Science: Processes & Impacts.* <https://doi.org/10.1039/d0em00446d>.
- Weiss, L., Ludwig, W., Heussner, S., Canals, M., Ghiglione, J.-F., Estournel, C., Constant, M., Kerhervé, P., 2021. The missing ocean plastic sink: gone with the rivers. *Science* 373, 107–111. <https://doi.org/10.1126/science.abe0290>.
- Woodall, L.C., Sanchez-Vidal, A., Canals, M., Paterson, G.L.J., Coppock, R., Sleight, V., Calafat, A., Rogers, A.D., Narayanaswamy, B.E., Thompson, R.C., 2014. The deep sea is a major sink for microplastic debris. *R. Soc. Open Sci.* 1 <https://doi.org/10.1098/rsos.140317>.
- Zheng, B., Chevallier, F., Yin, Y., Ciais, P., Fortems-Cheiney, A., Deeter, M.N., Parker, R. J., Wang, Y., Worden, H.M., Zhao, Y., 2019. Global atmospheric carbon monoxide budget 2000–2017 inferred from multi-species atmospheric inversions. *Earth Syst. Sci. Data* 11, 1411–1436. <https://doi.org/10.5194/essd-11-1411-2019>.
- Zhu, L., Zhao, S., Bittar, T.B., Stubbins, A., Li, D., 2020. Photochemical dissolution of buoyant microplastics to dissolved organic carbon: rates and microbial impacts. *J. Hazard. Mater.* 383 <https://doi.org/10.1016/j.jhazmat.2019.121065>.